

# The role of the atmospheric-pressure dielectric barrier discharge regime on the fragmentation of a cyclic siloxane precursor

J. Profili<sup>1</sup>, A. Durocher-Jean<sup>1</sup>, Ivàn Rodríguez<sup>2,3</sup>, G. Laroche<sup>2,3</sup>, and L. Stafford<sup>1</sup>

<sup>1</sup>Laboratoire de physique des plasmas, Département de physique, Université de Montréal, Montréal, Québec, Canada

<sup>2</sup>Laboratoire d'Ingénierie de Surface, Centre de Recherche sur les Matériaux Avancés, Département de Génie des Mines, de la Métallurgie et des Matériaux, Université Laval, Québec, Québec, Canada

<sup>3</sup>Centre de Recherche du Centre Hospitalier Universitaire de Québec, Hôpital St-François d'Assise, Québec, Québec, Canada

**Abstract:** Fourier transform infrared spectroscopy (FTIR) is used to investigate the link between the chemical properties of plasma-deposited thin films obtained in a plane-to-plane dielectric barrier discharge (DBD) and the fragmentation kinetics of the cyclic tetramethylcyclotetrasiloxane precursor. A strong modification of the OH functional groups deposited on the surface is observed between experiments obtained in glow regime (He carrier gas) and Townsend regime (N<sub>2</sub> carrier gas).

**Keywords:** Dielectric Barrier discharge, Atmospheric pressure, TMCTS, He, N<sub>2</sub>, FTIR.

## 1. Introduction

Dielectric Barrier Discharges (DBDs) at atmospheric-pressure have already demonstrated their ability for the synthesis of thin film with various micro and macroscopic properties [1]–[3] over a wide variety of commercial and/or unconventional substrates [4]–[6]. In many cases, the experiments are realized in rare gases such as helium or argon [7]–[9] to obtain homogeneous glow discharges. N<sub>2</sub>-based discharges operated in a Townsend regime [10] are also used for plasma enhanced chemical vapour deposition (PEDVD) and generally provide a much less expensive approach for industrial applications [11]. Depending on the carrier gas, and thus the discharge regime, significant change in the population of active species (ions, electrons, metastables, etc.) involved in PECVD are expected [11]. Although such difference are already well documented in literature, only a few studies have analyzed the influence of the discharge regime on the plasma deposition dynamics of functional thin films. The aim of this work is to investigate the chemical properties of siloxane-based coatings obtained in either Townsend (N<sub>2</sub>) or glow (He) discharges. Based on this set of data, the influence of the discharge regime on the precursor fragmentation is discussed.

## 2. Experimental section

### A. Reactor

Experiments were performed in a plane-to-plane DBD enclosed in a vacuum chamber. The DBD cell is formed by two electrodes (2.5 cm × 5.5 cm) made of metallized paint (Pt-Ag alloy) and deposited on alumina plates (635 μm thick). The glass substrate (75 mm × 115 mm, 2 mm thick, Multiver) was placed on the lower DBD electrode. The gas gap was set to 1 mm using two glass plates. The gas

mixture was continuously injected from one side of the DBD cell and constant atmospheric pressure was achieved through a gentle pumping of the vessel.

### B. Thin film deposition

The films were deposited from 2,4,6,8-tetramethylcyclotetrasiloxane (TMCTS, 99.5% purity, Sigma-Aldrich). The liquid precursor was injected into the system along the gas flow lines using a vapour source controller (Bronkhorst) coupled with a mass flow meter. All experiments performed in this work were realized using 3 SLM of He (5 UHP, Praxair) or N<sub>2</sub> (4.3 HP, Praxair) and the concentration of the polymerizable vapours are varied between 0 and 20 ppm. In addition, few ppm of O<sub>2</sub> (4.8 UHP, Praxair) are injected into the system as oxidizing gas.

The discharge was sustained by applying a sinusoidal electrical signal at a frequency of 12 kHz for He discharges and 3 kHz for N<sub>2</sub> discharges and a peak-to-peak voltage in the kV range. The power absorbed or dissipated in the glow or Townsend discharge was controlled by detailed measurements of the current-voltage characteristics. Such analysis was performed using a TDS2014C Tektronics oscilloscope (100 MHz, 2 GS/s) coupled with a high-voltage probe (75 MHz bandwidth) connected to the high-voltage electrode and a current toroid probe (100 MHz bandwidth) placed after the electrical load. For all experiments, the absorbed or dissipated power was maintained at 10 mW/cm<sup>2</sup>.

### C. Characterization of the thin film

The chemical composition of the plasma-deposited coatings was investigated by Attenuated Total Reflectance Fourier Transform Infrared spectroscopy (ATR-FTIR) in the 500 to 4 000 cm<sup>-1</sup> wavenumber range using a Bruker Vertex 70 spectrometer. All spectra are acquired by

averaging 30 scans with a spectral resolution of about  $4\text{ cm}^{-1}$ . A profilometer (KLA-Tencor Alpha-Step IQ Surface Profiler) was also used to estimate the thickness of the plasma-deposited coatings.

### 3. Results and discussion

Fig. 1 compares the ATR-FTIR spectrum of glass substrates before and after treatment in He/O<sub>2</sub>/TMCTS plasmas. The signature of the untreated sample is dominated by a wide band centered at  $\sim 900\text{ cm}^{-1}$  associated to the bending of the Si-OH groups ( $900\text{-}930\text{ cm}^{-1}$ ). This peak is superimposed to the wide asymmetric vibration of the Si-O-Si band ( $1000\text{-}1200\text{ cm}^{-1}$ ). After treatment, the maximum appears at  $1000\text{ cm}^{-1}$  with a shoulder at  $1100\text{ cm}^{-1}$ . This means that the signature of the substrate spectrum on the treated surfaces remains small; this is linked to the relatively high thickness of the plasma-deposited thin film (depth penetration of the ATR analysis with a diamond crystal is close to  $1.5\text{ }\mu\text{m}$ ). This result is also confirmed by measurements of the coatings thickness obtained by profilometry (between  $0.5$  and  $3\text{ }\mu\text{m}$  after the scratch test).

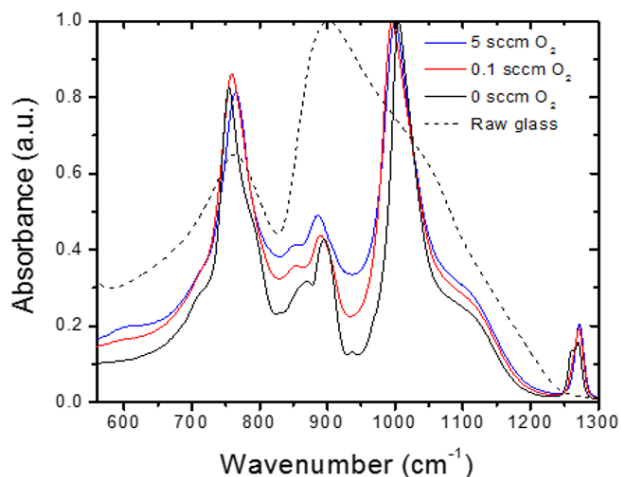


Fig. 1: ATR-FTIR spectrum ( $500\text{-}1300\text{ cm}^{-1}$  range) of glass substrates obtained after treatments in He/O<sub>2</sub>/TMCTS plasmas.

The addition of a small amount of oxygen ( $0.1\text{ sccm}$ ) during the deposition process in He/TMCTS plasmas leads to an extinction of the small peak at  $935\text{ cm}^{-1}$ . Similarly, oxidation reactions induce the extinction of the shoulder close to the  $1270\text{ cm}^{-1}$  peak associated to Si-CH<sub>3</sub> bonds. The presence of oxygen also leads to a shoulder close to  $600\text{ cm}^{-1}$  linked to the symmetric stretching mode of Si-O-Si groups; this band is strongly influenced by the molecule conformation in the coating. Some modifications are also observed between  $800$  et  $900\text{ cm}^{-1}$  and can be related to the modification of the symmetric stretching of the SiO-CH<sub>3</sub> with the bending of OSi-H and the Si-OH bending. The most significant change arising after injection of oxygen in He/TMCTS plasmas is observed in the  $1500\text{-}3500\text{ cm}^{-1}$  range (Fig. 2). In particular, the Si-H stretching mode at

$2170\text{ cm}^{-1}$  is strongly reduced while the small peak at  $2230\text{ cm}^{-1}$  remains almost unchanged.

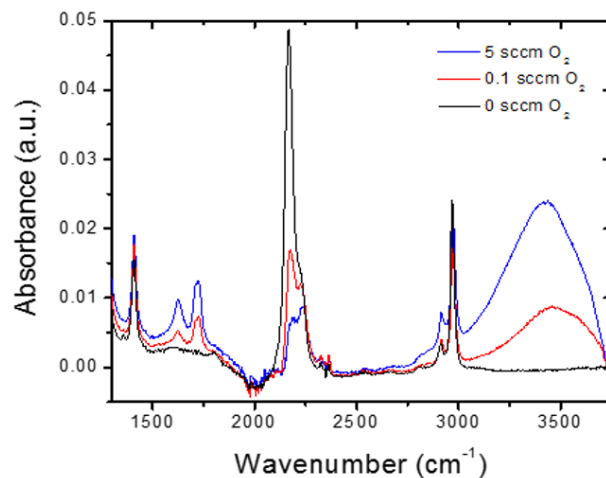


Fig. 2: ATR-FTIR spectrum ( $1300\text{-}3750\text{ cm}^{-1}$  range) of glass substrates obtained after treatments in He/O<sub>2</sub>/TMCTS plasmas.

With the augmentation of the O<sub>2</sub> concentration fraction in the discharge, different chemicals groups are also formed in the coating. More precisely, the  $1635$  and  $1735\text{ cm}^{-1}$  peaks can be linked to amide and aldehyde C=O bonds. The ratio between these vibrations varies with the amount of O<sub>2</sub> used during deposition: a higher amount of O<sub>2</sub> favors the creations of aldehydes groups. In addition, for higher surface oxidation, the amount of bonded hydroxyl groups seems be more important. Indeed, the band between  $2800$  and  $3750\text{ cm}^{-1}$  linked to the vibration of the Si-OH bond strongly increases with the O<sub>2</sub> concentration.

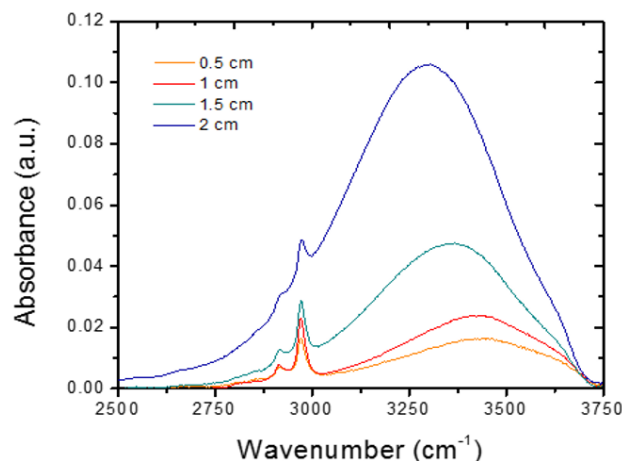


Fig. 3: ATR-FTIR spectrum ( $2500\text{-}3750\text{ cm}^{-1}$  range) of glass substrates obtained after treatments in He/O<sub>2</sub>/TMCTS plasmas as a function of position from the entrance ( $0.5\text{ cm}$ ) to the exit ( $2\text{ cm}$ ).

However, the strong vibration of the C-H<sub>x</sub> bonds observed between 2850 and 2950 cm<sup>-1</sup>, the bending of the C-H<sub>3</sub> bonds detected at 1413 cm<sup>-1</sup>, and the high peak linked to Si-CH<sub>3</sub> bonds at 1270 cm<sup>-1</sup> indicate that even for the higher oxygen concentrations, the amount of carbon in the coating remains fairly constant. Further FTIR analysis in the 2500 et 3750 cm<sup>-1</sup> range with respect to the position in the reactor along the gas flow lines (Fig. 3) indicate a modification of the chemical gradient as already observed in previous works [4]. This is related to the different residence times of the precursor in the discharge. In this case, FTIR spectra reveal an increase of the O-H band with the position along the gas flow line. In comparison, the intensity of the C-H<sub>x</sub> peaks slightly decreases. This means that the augmentation of the oxidation of the surface is linked to an increase of the residence time of the cyclic precursor in the He/TMCTS/O<sub>2</sub> discharge.

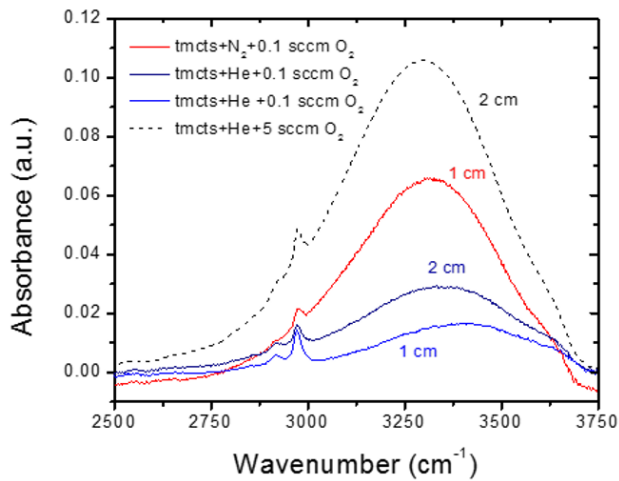


Fig. 4: Comparison between the ATR-FTIR spectrum of glass substrates in Townsend and glow discharges.

Fig. 4 shows a comparison between the ATR-FTIR signature in the 2500-3750 cm<sup>-1</sup> range for the thin films obtained in He (glow discharge) and N<sub>2</sub> (Townsend discharge). The main difference is the modification of the chemical gradient as a function of the residence time of the precursor. Indeed, in N<sub>2</sub>-based discharges, the maximum of the hydroxyls groups is observed closer to the entrance of the discharge (1 cm) where in He-based plasmas it was further (2 cm). This highlights a different fragmentation kinetics in glow versus Townsend discharges. Further analysis of the FTIR spectra indicates that an higher amount of hydroxylic groups are created in the coating with a Townsend discharge than in the glow discharge. Indeed, the results show that in order to obtain more OH groups in the coating in He-based plasmas, it is necessary to increase by approximately 50 times the amount of oxidizing species in the gas mixture. Also, the amount of the carbon moiety observed in the 2850-2950 cm<sup>-1</sup> range is reduced in the Townsend discharge. This is confirmed by

the similar reduction observed for the peak at 1270 cm<sup>-1</sup> (not show here).

The differences observed between the coatings obtained in He- versus N<sub>2</sub>-containing discharges can most likely be explained by the differences in the discharge physics. One of these aspects is linked to the I-V characteristics displayed in Fig. 5 (He) and Fig. 6 (N<sub>2</sub>). While a strong (7 mA) and narrow (5 μs) current peak is observed in the glow He discharge, a lower (1.3 mA, 5 times lower) but much wider current peak (60 μs, 12 times larger) is achieved in the Townsend N<sub>2</sub> discharge.

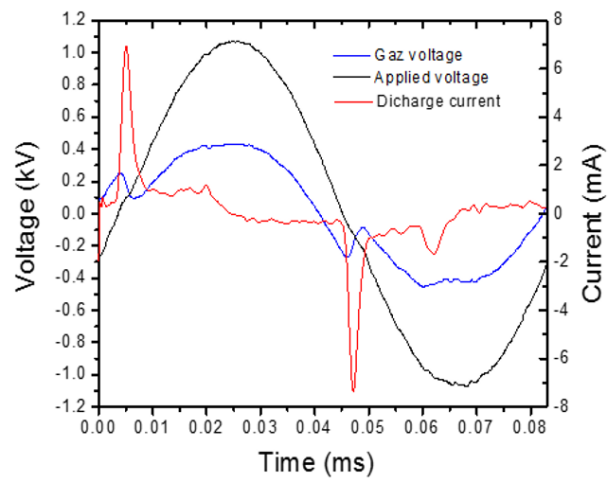


Fig. 5: Electricals characteristics from He discharge with a glass substrate (2.15 kV<sub>cc</sub>, 12 kHz, 10 mWcm<sup>-2</sup>).

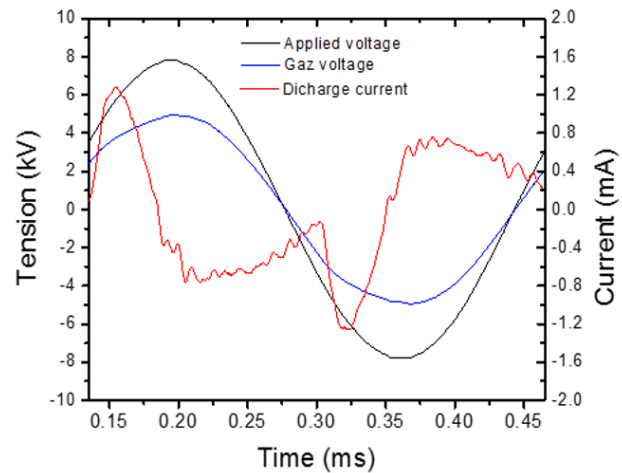


Fig. 6: Electricals characteristics from N<sub>2</sub> discharge with a glass substrate (15.6 kV<sub>cc</sub>, 3 kHz, 10 mWcm<sup>-2</sup>).

The second aspect is related to the populations of plasma-generated species (ions, electrons, and metastables). While these quantities were not explicitly measured in this work, simulations reported in the literature indicate that He glow discharges are characterized by electron number densities between 10<sup>10</sup> and 10<sup>11</sup> cm<sup>-3</sup> whereas these values for

Townsend N<sub>2</sub> discharges are between 10<sup>7</sup> and 10<sup>8</sup> cm<sup>-3</sup> for comparable ion number densities (between 10<sup>10</sup> and 10<sup>11</sup> cm<sup>-3</sup>) [11]. In addition, cycle-averaged electron temperatures (assuming Maxwellian electron energy distribution functions) are generally around 0.2 eV for glow He discharges [12] and above 1 eV for Townsend N<sub>2</sub> discharges [13]. Both of these features are expected to play an important role on the precursor fragmentation kinetics and thus on the nature of plasma-generated fragments. The lower carbon content obtained in the Townsend regime over the whole range of oxygen concentration fractions investigated thus suggests that for the TMCTS precursor, such features can be achieved in discharges characterized by high electron temperatures but low electron number densities.

#### 4. Conclusion

In summary, the FTIR analysis presented in this proceeding indicate a modification of the fragmentation dynamics of the cyclic precursor TMCTS with the addition of oxygen in glow He discharges. However, the results show a residuals carbon moiety even for high oxygen concentration fractions. A modification of the discharge regime from glow to Townsend discharge using N<sub>2</sub> as the carrier gas reveals a different fragmentation patterns of the precursor. This can most likely be linked to a change in the populations of high-energy electrons responsible for precursor fragmentation.

#### 5. References

- [1] D. W. Sheel and J. L. Hodgkinson, "Atmospheric-Pressure Glow Discharge CVD of Composite Metallic Aluminium Thin Films," *Plasma Process. Polym.*, vol. 4, no. 5, pp. 537–547, Jul. 2007.
- [2] Y. Suzaki *et al.*, "Deposition of ZnO film using an open-air cold plasma generator," *Thin Solid Films*, vol. 506–507, pp. 155–158, May 2006.
- [3] J. Bardon *et al.*, "Characterization of a plasma polymer coating from an organophosphorus silane deposited at atmospheric pressure for fire-retardant purposes," *Prog. Org. Coatings*, vol. 88, pp. 39–47, 2015.
- [4] J. Profili, O. Levasseur, N. Naudé, C. Chaneac, L. Stafford, and N. Gherardi, "Influence of the voltage waveform during nanocomposite layer deposition by aerosol-assisted atmospheric pressure Townsend discharge," *J. Appl. Phys.*, vol. 120, no. 5, 2016.
- [5] P. Favia, D. Pignatelli, G. Dilecce, B. R. Pistillo, M. Nardulli, and R. Gristina, "Stimulating living cells with air DBD plasma," in *MRS Proceedings*, 2012, no. 1469.
- [6] J. Profili, L. Levasseur, A. Koronai, L. Stafford, and N. Gherardi, "Deposition of nanocomposite coating on wood using atmospheric pressure cold discharge," *Surf. Coatings Technol.*, vol. In Press, 2016.
- [7] O. Levasseur *et al.*, "Deposition of Hydrophobic Functional Groups on Wood Surfaces Using Atmospheric-Pressure Dielectric Barrier Discharge in Helium-Hexamethyldisiloxane Gas Mixtures," *Plasma Process. Polym.*, vol. 9, no. 11–12, pp. 1168–1175, Dec. 2012.
- [8] F. Fanelli, F. Fracassi, and R. d'Agostino, "Deposition of Hydrocarbon Films by Means of Helium-Ethylene Fed Glow Dielectric Barrier Discharges," *Plasma Process. Polym.*, vol. 2, no. 9, pp. 688–694, Nov. 2005.
- [9] M. Laurent, J. Koehler, G. Sabbatier, C. A. Hoesli, N. Gherardi, and G. Laroche, "Atmospheric Pressure Plasma Polymer of Ethyl Lactate : In Vitro Degradation and Cell Viability Studies," *Plasma Process. Polym.*, vol. 13, pp. 711–721, 2016.
- [10] J. Profili, O. Levasseur, J. Blaisot, A. Koronai, L. Stafford, and N. Gherardi, "Nebulization of Nanocolloidal Suspensions for the Growth of Nanocomposite Coatings in Dielectric Barrier Discharges," *Plasma Process. Polym.*, vol. 13, no. 10, pp. 981–989, 2016.
- [11] F. Massines, C. Sarra-Bournet, F. Fanelli, N. Naudé, and N. Gherardi, "Atmospheric Pressure Low Temperature Direct Plasma Technology: Status and Challenges for Thin Film Deposition," *Plasma Process. Polym.*, vol. 9, no. 11–12, pp. 1041–1073, Dec. 2012.
- [12] O. Levasseur, K. R. Gangwar, J. Profili, N. Naudé, N. Gherardi, and L. Stafford, "Influence of substrate outgassing on the plasma properties during wood treatment in He dielectric barrier discharges at atmospheric pressure," *Plasma Process. Polym.*, no. November, pp. 1–7, 2016.
- [13] J. Prigent *et al.*, "Determination of active species in the modification of hardwood samples in the flowing afterglow of N<sub>2</sub> dielectric barrier discharges open to ambient air," *Cellulose*, vol. 22, pp. 811–827, 2015.